face may be expected, owing to the relative flatness of curve for the neutron dose versus depth.

As pointed out by Wilson and Miller (*8*), the ratio of primary to secondary dose is greatly influenced by shield-target geometry and may therefore be quite different for space capsules than for a body within the atmosphere. Nevertheless, a rough estimate of the neutron dosage inside an aluminum-shielded space capsule during a solar particle event may be made from Figs. 2 through 5. The cross-section for neutron production in aluminum is approximately a factor of 1.7 times larger than the corresponding cross-section in air. If similar neutron scattering and absorption cross-sections in the two materials and similar geometry are assumed, the neutron dosage under a given thickness of aluminum shielding would then be roughly 1.7 times greater than the neutron dosage under the same thickness of atmosphere.

The proton dosage, on the other hand, is nearly independent of the composition of the shielding material over the range of elements from nitrogen to aluminum. Hence, the ratio of neutron to proton dosage would be higher under an aluminum shield than under an air shield with the same thickness and geometry.

The neutron and total proton dosages in rads and in rems at selected atmospheric depths are shown as a function of P_0 in Figures 3 and 4. With the aid of these curves, the total dose rate can be calculated as a function of time for any solar proton event for which the time variations of P_0 and $(dJ/dP)_0$ are known. This is illustrated in Fig. 5, which shows the time variations of P_0 and J_0, where $J_0 = P_0(dJ/dP)_0$, 12 to 16 November 1960 (*1*), together with the corresponding neutron and total proton dose rates at atmospheric depths of 1, 20, and 50 g/cm². Two 3+ solar flares occurred during the period in question, one at 1329 UT on 12 November and the second at 0221 UT on 15 November. Time-integrated dosages associated with each of the two flares are given in Table 1. The time-integrated neutron dosage exceeds the total proton dosage below atmospheric depths of 25 to 30 g/cm².

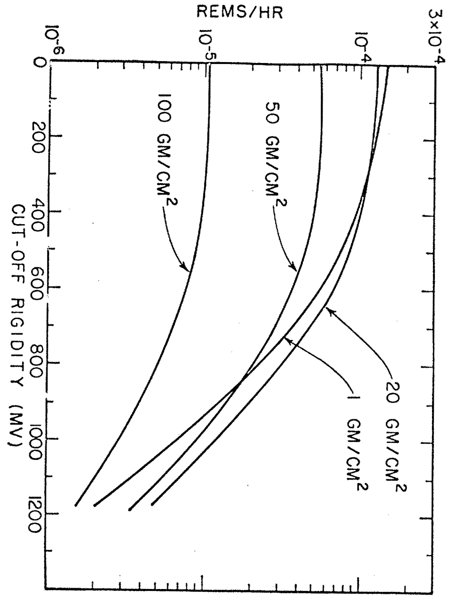

Fig. 6. Total neutron dosage in rads as a function of geomagnetic-cutoff rigidity. The solar proton spectrum $dJ/dP = (dJ/dP)_0 \exp(-P/125\text{Mv})$ normalized to $(dJ/dP)_0 = 1$ proton cm^{-2} sec^{-1} Mv^{-1}.

The variation of neutron dose rate with geomagnetic cutoff rigidity is shown in Fig. 6. The decrease in proton dosage with increasing cutoff rigidity occurs predominantly at high altitudes, whereas the decrease in neutron dosage is relatively evenly distributed over all atmospheric depths. Thus, the ratio of neutron to proton dose increases at high altitudes as the cutoff rigidity is raised. This is of interest in connection with shielding of high-altitude aircraft at low latitudes and of orbiting vehicles within the geomagnetic field.

In summary, the dosage from secondary neutrons produced by solar protons exceeds the dosage from primary and secondary protons at atmospheric depths greater than 30 g/cm². This is roughly the upper boundary at which projected supersonic aircraft can cruise (*9*). The neutron dosage falls by a factor of two between 30 and 50 g/cm² (between 24,000 and 21,000 meters) whereas the proton dosage falls by a factor of five over the same altitude range. Surface neutron dosages to persons flying a polar route at 24,000 meters during a major solar-particle event are of the order of 0.1 rem per hour at the peak of the event and 1 rem over the duration of the event. Such events occur about once a year during solar maximum.

Hence, the accumulated dose to pilots of supersonic aircraft appears to be below the maximum permissible level of 5 rems per year for chronic exposure (*3*). Further reduction of the total dosage can be accomplished most efficiently by shielding with materials having a high cross section for neutron absorption.

E. J. Flamm
R. E. Lingenfelter
Institute of Geophysics and Planetary Physics, University of California, Los Angeles

References and Notes

1. P. Freier and W. R. Webber, *Science* **142**, 1587 (1963); *J. Geophys. Res.* **68**, 1605 (1963).
2. R. E. Lingenfelter and E. J. Flamm, *J. Atmos. Sci.*, in press; *J. Geophys. Res.*, in press.
3. Natl. Bur. Std. (U.S.) Handbook 63, (1957).
4. M. Rich and R. Madey, *UCRL-2301*, Lawrence Radiation Laboratory, Berkeley, Calif. (March 1954).
5. S. J. Lindenbaum, *Ann. Rev. Nuclear Sci.* **11**, 213 (1961).
6. W. R. Webber and P. Freier, *TID-7652*, Book I, U.S. Atomic Energy Commission (1962).
7. H. Kallman-Bill, Ed., Cospar International Reference Atmosphere, 1961, (North-Holland, Amsterdam, 1961).
8. R. K. Wilson and R. A. Miller, *TID-7652*, Book II, U.S. Atomic Energy Commission (1962).
9. H. J. Schaefer, *Aerospace Med.* **34**, 1 (1963).
10. Publication No. 364, Institute of Geophysics and Planetary Physics, University of California, Los Angeles.

24 April 1964

Calcite-Aragonite Equilibrium at 100°C

Abstract. *The equilibrium pressure of the calcite-aragonite transition has been determined near 100°C and is 4.35 kilobars. These data are in agreement with earlier work but conflict with the most recent determination by Simmons and Bell.*

At low temperatures, the free energy of the calcite-aragonite transition is small [250 cal/mole, Latimer (*1*)] and direct experiments are necessary to fix the transition pressure with any degree of certainty. The low temperature data of Jamieson (*2*) and extrapolation of MacDonald's (*3*) and Clark's (*4*) data indicate a transition pressure of about 4.5 kb at 100°C. At low temperature, direct study is difficult because of the sluggish nature of the transition; but Dachille and Roy (*5*) and Simmons and Bell (*6*) were able to effect transitions in the range 25° to 100°C by using the oscillating squeezer. Dachille and Roy found the transition near 4 kb at 100°C. Simmons and Bell report the much higher value of 7 kb. In view of these discrepancies and the problems associated with the squeezer devices we

Table 1. Results of calcite-aragonite experiments: C, calcite; A, aragonite; parentheses denote minor phase. Starting materials: P, precipitated fine calcite and aragonite; M, metamorphic aragonite with minor calcite.

Temp. (°C)	Pressure (kb)	Starting material	Products	Time (days)
109	6.21	P	A	5
120	6.00	P	A+(C)	5
101	5.52	P	A+(C)	5
100	5.18	P	No change	5
110	5.00	P	A+(C)	5
100	4.14	P	C	5
107	4.48	P	A+(C)	14
100	4.83	P	A+(C)	17
115	4.14	P	C+(A)	17
98	4.48	M	A+(C)	20
105	4.14	M	C+(A)	20
105	4.83	M	A	29

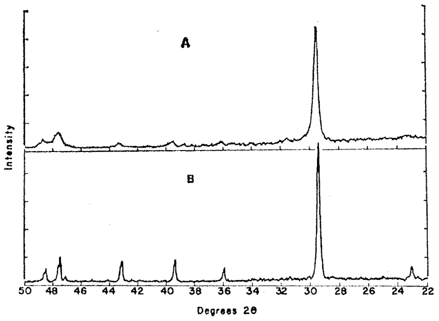

Fig. 1. Comparison of two x-ray diffraction patterns of a fine precipitated calcite. (*A*) After squeezing at 10 kb at room temperature. (*B*) Original material. Note the disappearance and broadening of the lines in *A*.

have repeated these studies in conventional hydrostatic apparatus.

The reaction was studied by placing mixtures of calcite and aragonite in small hot-seal vessels. A small amount of calcium chloride was added to each charge to give an approximately 0.2 molar solution. Calcium chloride greatly accelerates the rate of attainment of equilibrium in this reaction. Charges were brought to temperature dry, and then pumped to the desired pressure. Two starting materials were used and gave identical results. A mixture of fine calcite and aragonite was precipitated at 100°C from potassium carbonate and calcium chloride solutions. The second material was a sample of metamorphic aragonite supplied by R. G. Coleman and described in Coleman and Lee [(*7*), sample 45-CZ-59]. This material contains a small amount of calcite and about 1.11 percent strontium carbonate as the only major impurity. The material was ground to pass a 325-mesh screen. Phases produced and changes in relative quantities were determined by x-ray diffraction and optical observation. The data are given in Table 1. There was no evidence of any contamination of products by calcium chloride solutions nor do mineralogical data of Deer, Howie, and Zussman (*8*) indicate chloride solid solution in these phases.

Inspection of these data indicates a transition pressure between 4.2 and 4.5 kb at 100°C. The results are very close to those of Jamieson, MacDonald, and Clark and indicate that Simmons and Bell's transition pressure is much too high at this temperature.

Some observations on squeezer products are of interest in evaluating the significance of data derived from such apparatus where shearing stresses may be large. In Fig. 1 diffraction patterns are compared for a fine precipitated calcite (*B* in the figure) and the same material after squeezing at 10 kb at room temperature (*A*). The squeezed material shows intense line broadening, a result of some combination of grain size reduction and internal strain, the latter being associated with a large dislocation density. Aragonite squeezed at 10 kb also shows broadening of comparable magnitude. Paterson (*9*) has discussed line broadening in deformed calcite and suggested that the stored strain energy may be of the order of 1000 cal/mole. The broadening in Fig. 1 is far larger than that found by Paterson. The strain energy term may be much larger than the free energy of the calcite-aragonite transition and it may well be necessary to consider exactly what physical state of a system is being studied in shearing apparatus. It certainly does not appear to be that of hydrostatically stressed particles of reasonable grain size.

WILLIAM A. CRAWFORD
WILLIAM S. FYFE
Department of Geology and Geophysics, University of California, Berkeley

References and Notes

1. W. M. Latimer, *Oxidation Potentials* (Prentice Hall, Englewood Cliffs, ed. 2, 1952), p. 320.
2. J. C. Jamieson, *J. Chem. Phys.* **21**, 1385 (1953).
3. G. J. F. MacDonald, *Am. Mineralogist* **41**, 744 (1956).
4. S. P. Clark, Jr., *ibid.* **42**, 564 (1957).
5. F. Dachille and R. Roy, in *Reactivity of Solids,* J. H. De Boer, Ed. (Elsevier, Amsterdam, 1960), p. 502.
6. G. Simmons and P. Bell, *Science* **139**, 1197 (1963).
7. R. G. Coleman and D. E. Lee, *Am. J. Sci.* **260**, 588 (1962).
8. W. A. Deer, R. A. Howie, J. Zussman, *Rock-Forming Minerals* (Wiley, New York, 1963), vol. 5, pp. 232, 397.
9. M. S. Paterson, *Phil. Mag.* **4**, 451 (1959).
10. Supported by the Petroleum Research Fund of the American Chemical Society and the NSF.

13 April 1964

Strain-Induced Birefringence in Fluoride Films on Uranium Dioxide

Abstract. *Optically birefringent microstructures are formed within fluoride films that are produced on uranium dioxide by hydrofluorination. The positive molar volume change of the reaction produces nonuniform tensile and compressive stresses around sites of surface roughness which result in optical double refraction.*

Moyer and Ochs (*1*) have recently studied the optically birefringent spherulites within polymer films by microscopy and tritium autoradiography. Their photomicrographs taken with polarized light show superficial similarity to features also seen in surface films produced by gas-solid reactions. We have observed analogous doubly refractive microstructures within fluoride films formed on polished surfaces of uranium dioxide by hydrofluorination. These latter growth features appear to be the result of nonuniform lateral stresses originating within the film around sites of nonplanar surface topography (*2*).

Hydrofluorination reactions were performed in a nickel reaction chamber under controlled conditions of pressure, time, and temperature. The materials and apparatus were described earlier (*3*). The product films were examined on a Bausch and Lomb research metallograph and on a Zeiss metallurgical microscope. Figure 1*A* shows a photomicrograph taken with a bright-field illumination and a 5550-Å filter of a film 2 μ thick formed on a flat, polished surface of UO_2 (solid) by reaction with HF (gas) at 60 cm-Hg and 286°C for 90 hours. Nonuniformity of thickness is evident from the interference bands along the scratch and around the hillocks and pits. The smooth area is thicker than the surrounding regions so that the bands indicate a progressive thinning away from the flats. This was demonstrated by a tilt in the interference filter which shifts the transmitted wavelength from 5550 Å to the blue. The bands are thus observed to move away from the flats, and, in the case of the circular nonuniformities, to close in upon themselves. This observation was confirmed by the same tilt-shift in a wedge formed in the film by a scratch mark. Figure 1*B* shows the same area as in Fig. 1*A* but was photographed with crossed polarizers. Three distinct features can be correlated with Fig.